AEROSPACE RESEARCH COMMUNICATIONS
ORIGINAL RESEARCH
published: 02 March 2026
doi: 10.3389/arc.2026.15921

Ignition and Lean Blowout Performance of an Annular Mixed-Flow Trapped Vortex Combustor Under Sub-Atmospheric Pressure

Qihang Li[1], Ping Jiang[1,2], Hongchun He[1], Zejun Wu[1,2]* and Xiaomin He[3]*

[1]School of Power and Energy, Nanchang Hangkong University, Nanchang, China, [2]Engineering Research Center of Aero-Engine Technology for General Aviation, Ministry of Education, Nanchang, China, [3]College of Energy and Power Engineering, Nanjing University of Aeronautics and Astronautics, Nanjing, China

In this paper, ignition and lean blowout (LBO) performance of an annular mixed-flow trapped vortex combustor (MTVC) were investigated under sub-atmospheric pressure. Experimental investigations were conducted to evaluate the ignition and lean blowout (LBO) performance under various sub-atmospheric pressure conditions. The findings indicate that MTVC has excellent ignition performance, the ignition pressure of the combustor can reach 35.3 kPa under ambient temperature, and the corresponding altitude is close to 8,000 m. As the pressure drops, the range of ignitable velocities diminishes, leading to increase in ignition fuel to air ratio (FAR) and LBO FAR. These shifts can be attributed to the more challenging combustion conditions and heightened inlet velocity resulting from reduced pressure. Notably, the ignition and LBO performance see substantial enhancements with rising temperatures. However, the positive impact of elevated temperature hardly compensated for the detrimental impact of lower pressure on ignition. There is minimal noticeable impact of the inlet Mach number on the ignition and LBO performance. Numerical simulations are carried out for both unreactive and reactive flow to verify the experiment results.

Keywords: mixed-flow trapped vortex combustor, sub-atmospheric pressure, ignition, lean blowout, fuel to air ratio

***Correspondence**
Ping Jiang,
jiangping924@nchu.edu.cn
Zejun Wu,
wuzejun9527@outlook.com

Received: *19 November 2025*
Accepted: *06 February 2026*
Published: *02 March 2026*

Citation:
Li Q, Jiang P, He H, Wu Z and He X (2026) Ignition and Lean Blowout Performance of an Annular Mixed-Flow Trapped Vortex Combustor Under Sub-Atmospheric Pressure. Aerosp. Res. Commun. 4:15921. doi: 10.3389/arc.2026.15921

INTRODUCTION

Aircraft engines must have the capability to restart while in flight at high altitudes, primarily for safety reasons. Initiating a startup at an altitude of 6,000 m, where ambient pressure can be as low as 47 kPa, presents one of the most challenging scenarios [1]. It is widely accepted that for every 100 m of altitude gained, both air temperature and pressure decrease by approximately 0.6 K and 0.786 kPa, respectively. According to a NASA report, combustion pulsation with significant noise occurs at altitudes above 6,000 m and atmospheric pressures below 47 kPa, leading to closely spaced Lean Blowout (LBO) and rich blowout limits [2]. Additionally, poor atomization due to sub-atmospheric pressure and low temperature exacerbates the challenges of re-ignition [3]. Hence, it is imperative to understand ignition performance and LBO limits at high altitudes with sub-atmospheric pressure to enhance overall aeroengine performance.

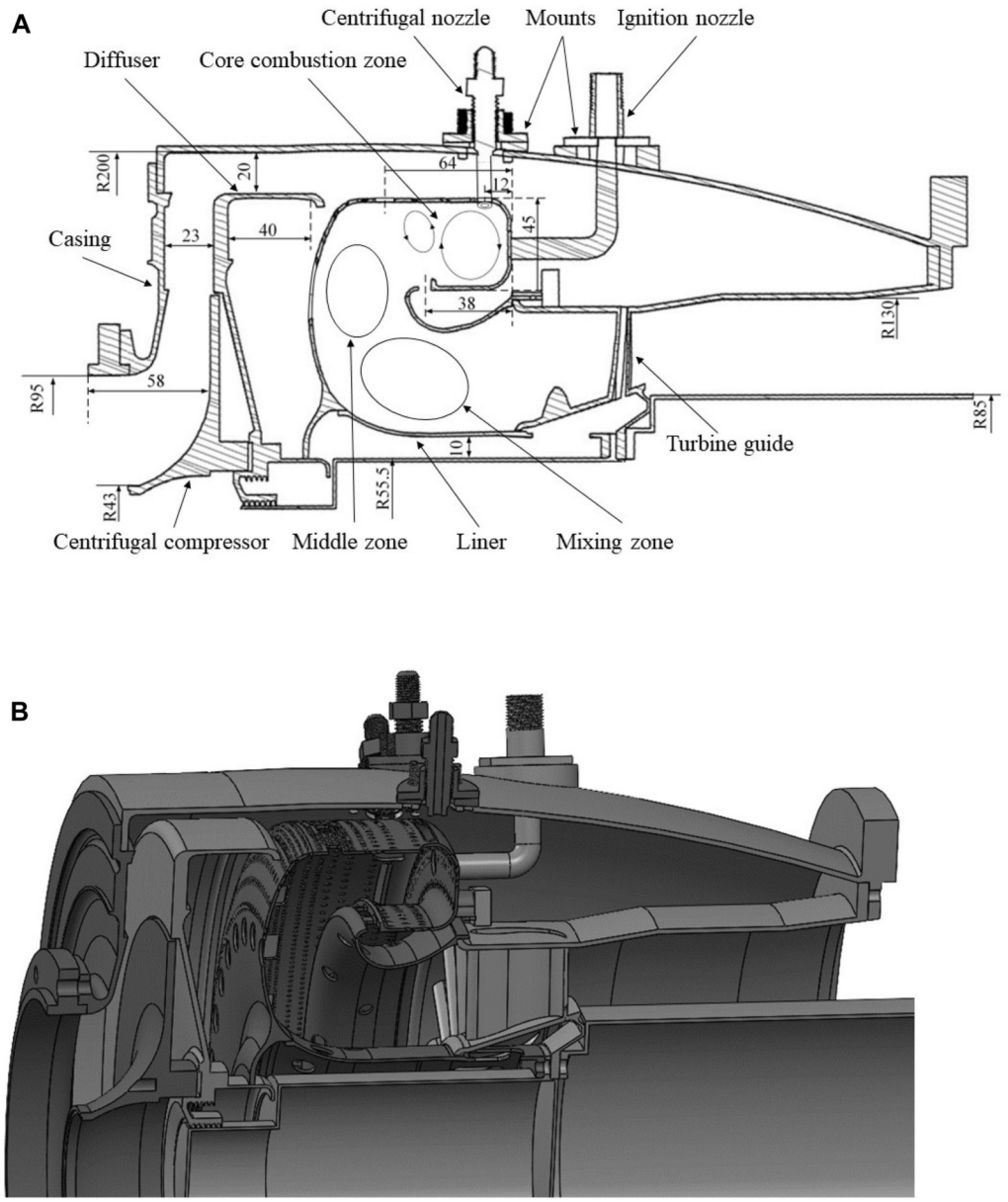

FIGURE 1 | 2D and 3D structure diagrams of MTVC. **(A)** 2D structure diagram. **(B)** 3D structure diagram.

A preliminary investigation of the ignition capability of the reverse-flow combustor was conducted under low-pressure conditions by Okai et al. [4]. The study revealed that lower pressure conditions made ignition more challenging, resulting in reduced ignitable inlet flow and reference velocity. Linassier et al. [1] examined the ignition and LBO performance of a multi-sector combustor under high-altitude conditions. They observed that under low temperatures and pressures, LBO limits were slightly higher than ignition limits. He et al. [5] explored lean-rich fuel ignition limits and ignition delay times of a catalytic igniter in an afterburner under low-pressure conditions ranging from 0.04 to 0.12 MPa. Their findings indicated that as pressure decreased, the range of ignitable velocities narrowed, ignition delay times increased, and the fuel to air ratio (FAR) of the lean ignition limit expanded. According to their theories, air becomes diluted at low pressures, resulting in reduced rates of chemical reactions on the catalyst surface. Numerous researchers have conducted combustion experiments at high altitudes with low pressure, highlighting characteristics such as a slow combustion rate, low combustion efficiency, low flame temperature, small flame width, and low flame height [6–13].

Trapped Vortex Combustor (TVC) is an innovative combustion technique for aviation engines that has recently

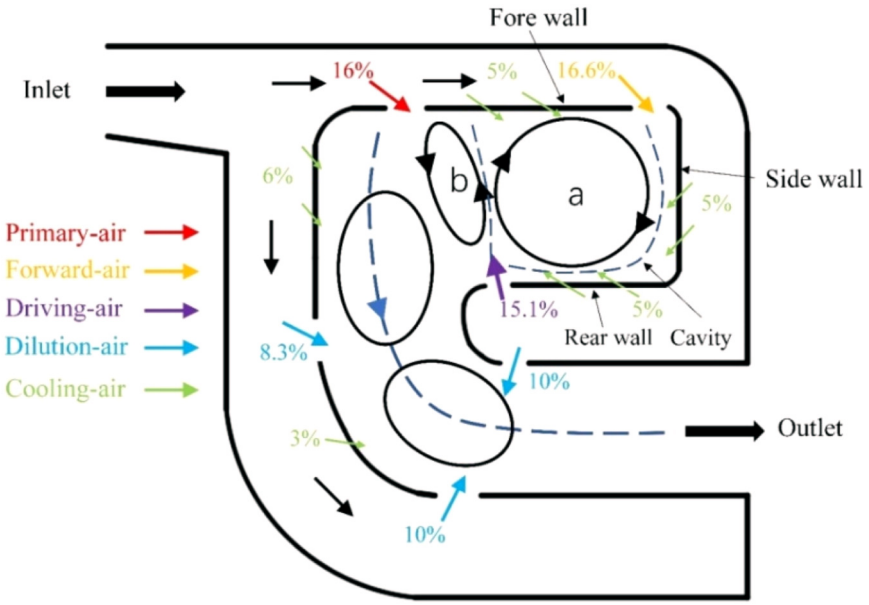

FIGURE 2 | Airflow distribution of MTVC.

been developed. It utilizes trapped vortex technology, which has garnered increasing interest due to its excellent combustion properties and low pollutant emissions. The TVC features a concave cavity structure and a main combustion area, enabling graded combustion in different engine states. It efficiently reduces emissions, including nitrogen oxides.

The igniter of TVC is situated in the concave cavity area, ensuring superior ignition performance and resistance to blowout compared to other combustors [14, 15]. A well-designed cavity in a TVC creates a stable reflow zone over a wide operating range, enhancing combustion stability [14, 16]. Under specific conditions, it can form a double anti-rotating vortex within the cavity, remaining undisturbed by the main flow even at high inlet velocities [17–20]. Research on TVCs has yielded significant benefits for engine performance, including: 1) Extending the useful combustion efficiency range by 40% to over 99%; 2) Improving ignition, blowout, and relight performance by 50%; 3) Reducing NOx emissions by a factor of 5.5 compared to the 1996 ICAO requirement for advanced commercial engine cycles; 4) Offering a 40% larger working range than typical combustors [15, 21–23]. TVCs find widespread applications in primary combustors [24–26], afterburners [27], inter-turbine burners [28–31], ultra-compact combustors [32–36], and low-emission combustors [37–39]. (These characteristics make TVCs stand out as energy-saving and energy-conversion technologies. Recent studies on flame stabilization and cooling designs, such as those involving air-cooled bluff-body flameholders and jet-cooled wall flameholders, further highlight the importance of thermal management and flow control in maintaining combustion stability under extreme conditions [40, 41]).

An innovative turboshaft combustor, named mixed-flow trapped vortex combustor (MTVC), was developed and showcased in previous research conducted by the group. The MTVC was examined through a three-dome sector test bench, investigating aspects such as flow distribution, flow field characteristics, fuel-air arrangement, and structural attributes [15, 20, 21]. Sub-atmospheric pressure conditions refer to pressures below the standard atmospheric pressure at sea level (101.3 kPa or 1 atm). When operating a combustion system under sub-atmospheric pressure conditions, several factors can come into play that might influence the ignition and lean blowout performance of MTVC. The primary focus of this paper lies in experimentally validating the performance of the annular MTVC. The central objective is to assess ignition capability and lean blowout (LBO) performance through testing the annular MTVC within a high-altitude, sub-atmospheric pressure environment. The outcomes of this paper will serve as valuable reference for design and construction of combustors intended for turboshaft applications at elevated altitudes in the future.

EXPERIMENT DESCRIPTION

Experiment Model

The MTVC described in this paper departs from normal TVC by incorporating axially graded combustion and rich-quench-lean (RQL) combustion design techniques. The detailed concept of the MTVC is described in Ref. [21]. In this work the MTVC was designed as an annular. The construction is comprised of the casing, axial diffuser, liner, mounts, centrifugal nozzle, ignition nozzle and turbine guide, as shown in **Figure 1**.

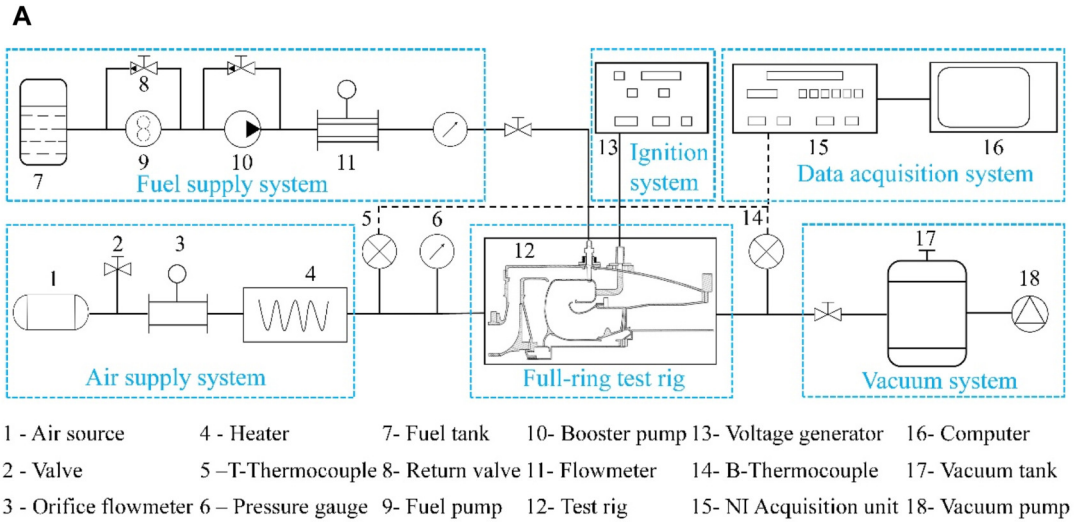

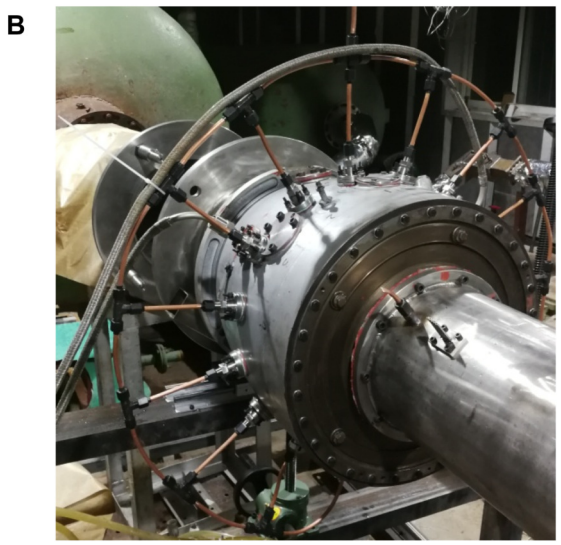

FIGURE 3 | Experiment system and Photograph of experimental scene. **(A)** Experiment system. **(B)** Photograph of experimental scene.

To withstand the elevated temperatures generated during combustion, the liner is precision-machined from a 1 mm thick super alloy (GH3044). Positioned at the front of the casing, the centrifugal compressor is attached, while the turbine guide is affixed to the rear. An axial diffuser, situated within the front of the casing, is employed for the centrifugal compressor. As high-pressure air enters the combustor from the axial diffuser of the centrifugal compressor, it divides into two primary streams: the first stream is utilized for combustion, and the second stream serves for supplementary combustion and mixing, as depicted in **Figure 2**. The combustor is categorized into three zones based on the air inlet: the core combustion zone, middle zone, and mixing zone. The core combustion zone, responsible for ignition and flame stability, results from the reciprocal interaction between primary air and cavity air. The annular air from the cooling and mixing holes in the casing wall enters the combustor to create the middle and mixing zones. The mixing zone is employed to regulate the exit temperature field, while the middle zone supports supplementary combustion. The cooling holes are arranged in a staggered pattern, incorporating multiple rows of cooling air inlet holes on both the cavity wall and the mainstream area wall. This design offers dual benefits: protection against high-temperature ablation of the wall surface and the uniform distribution of temperature at the combustor outlet. To

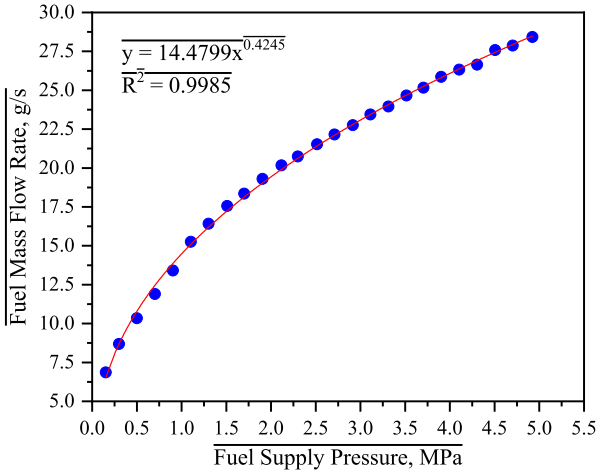

FIGURE 4 | The variation of fuel flow rate with fuel supply pressure.

TABLE 1 | Detailed RP-3 kerosene properties based on GB/T test method.

Property	Specification limits	RP-3 kerosene	Test methods
Density at 20 °C, kg/m^3		775 to 840	GB/T 1884 or GB/T 1885
Net heat of combustion, MJ/kg	min	42.8	GB/T 384
Viscosity at 20 °C, mm^2/s	min	1.25	GB/T 265
Flash point, °C	min	38	GB/T 261
Freezing point, °C		−47	GB/T 0197
Final boiling point, temperature, °C	Max	300	GB/T 255

accommodate the centrifugal nozzle, there are 15 evenly spaced nozzle assembly mounts positioned above the central section of the casing. Fuel is injected in the same direction as the forward airflow, facilitating its evaporation. On each side of the rear part of the casing, there is an ignition mount for securing the ignition nozzle. The igniter is positioned in proximity to the side wall where the local FAR is high and the airflow velocity is low, making it an optimal location for ignition.

Figure 2 illustrates the double-vortex flow structure and airflow distribution within the MTVC. Driving-air makes up 15.1% of the combustor airflow and forward-air makes up 16.6% to improve the combustion efficiency and flame stability. The primary-air makes up 16% of the combustor airflow to achieve complete combustion reaction and close the return zone in the cavity. The dilution-air makes up 28.3% of the combustor airflow to regulate the outlet temperature distribution. The cooling-air makes up 24% of the combustor airflow will be used to better protect the combustor.

When the driving-air encounters the cavity, a portion of it is deflected to the right, mixing with fresh forward-air to form the primary vortex (see in **Figure 2A**) within the cavity. Simultaneously, another portion is deflected to the left, merging with the primary-air to create the secondary vortex (see in **Figure 2B**) within the cavity. As a result of this configuration, a double-vortex flow structure is established, featuring the primary vortex rotating in one direction and the secondary vortex circulating in the opposite direction. The presence of the secondary vortex serves to protect the primary vortex from the impact of the primary-air, enhancing the stability of the primary vortex. Furthermore, it enhances combustion efficiency by facilitating the transfer of heat and mass between the trapped vortex zone and the mainstream zone. This intricate flow pattern contributes to optimized combustion within the MTVC.

TABLE 2 | Working conditions of MTVC.

Parameters / Programs	P (kPa)	T (K)	Ma
Condition 1	35.3, 41.3, 51.3, 61.3, 71.3, 81.3, 101.3	300	0.045–0.1
Condition 2	35.3–350	290	0.075
Condition 3	51.3, 61.3, 101.3	283–500	0.1

TABLE 3 | Instrument error in inlet parameters measurement.

Measurement device	Function	Accuracy (%)
Orifice flowmeter	Inlet flow rate	1
T thermocouple	Inlet temperature	0.4
NI acquisition unit	Collecting the inlet temperature data	0.5
Pressure gauge	Inlet pressure	0.4

Experiment Setup and Conditions

Figure 3 depicts the experimental system and a photograph of the experimental scene, including air supply system, fuel supply system, ignition system, data acquisition system and vacuum system.

The air supply system supplies air to the combustor through three screw compressors, with each compressor capable of delivering up to 34.4 m^3/min of mass flow. The air mass flow rate is measured using an orifice flowmeter with a 1% margin of error and is controlled by a regulating valve. Before reaching the test stand, the air is heated to a temperature of 523 K by an electric heater. The inlet temperature of the combustor is measured using a T-thermocouple with an error of 0.4% within the range of 73 K–673 K, ensuring precise control of the necessary mass flow rate and inlet air temperature. Meanwhile, a B-thermocouple is employed to measure the outlet temperature of the combustor, with an error of 0.4% within the range of 273 K–1573 K. The ignition results can be distinguished by observing the outlet temperature.

The vacuum system consists of vacuum tank and vacuum pump. The vacuum system provides a stable vacuum environment for the experiment. For the sub-atmospheric pressure experiment, air in the vacuum tank is pumped by three vacuum pumps. In the experimental, a regulating valve regulates the necessary sub-atmospheric pressure. The vacuum level can be as low as 20 kPa at air mass flow rate of 1 kg/s.

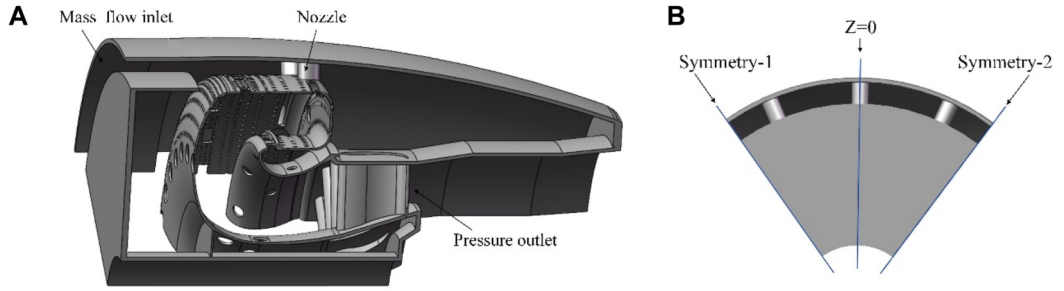

FIGURE 5 | Computational domain and boundary conditions. **(A)** Side view. **(B)** Main view.

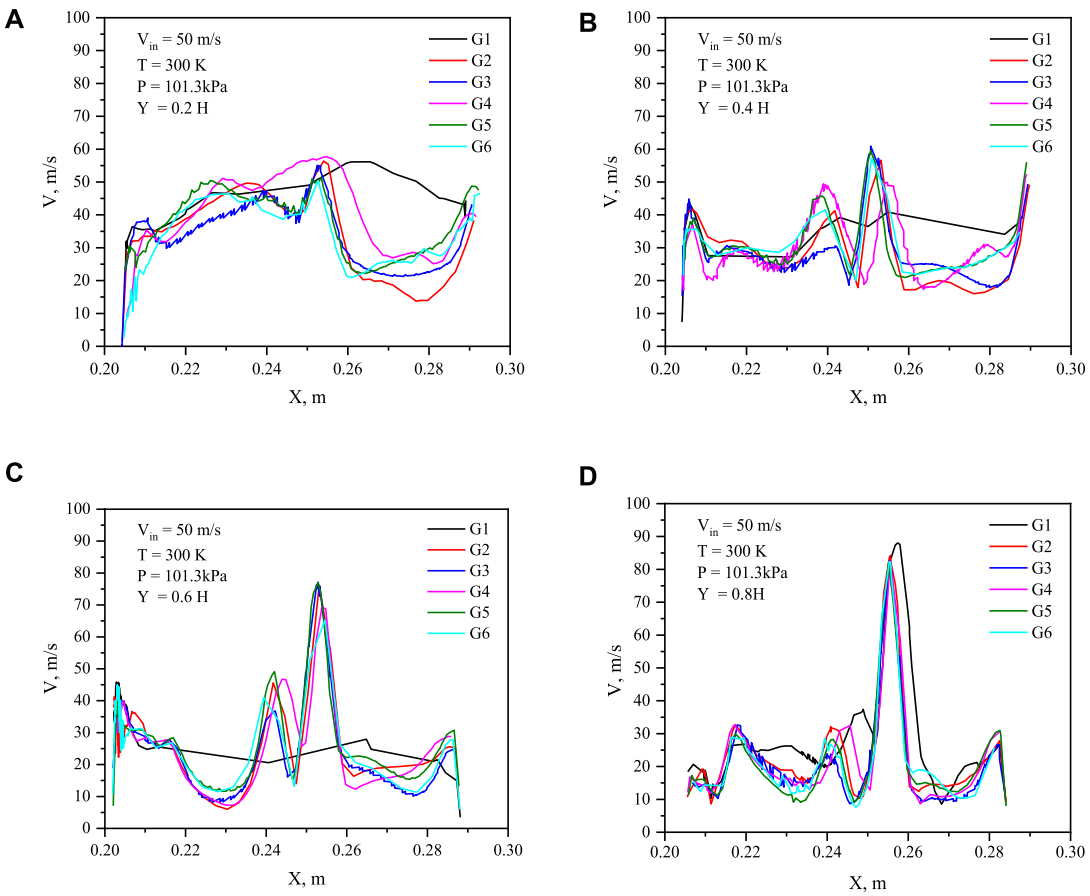

FIGURE 6 | The velocity distributions in different height directions. **(A)** Y = 0.2H. **(B)** Y = 0.4H. **(C)** Y = 0.6H. **(D)** Y = 0.8H.

The fuel supply system comprises a fuel tank, fuel pump, and booster pump. The fuel injection pressure and volume to the nozzles are adjusted by regulating the valve's opening while reducing the opening of the return valve. A flowmeter with a 1% margin of error measures mass flow rate of the fuel. Annular MTVC features fifteen centrifugal nozzles for fuel injection, each with cone angle of 80° and flow number of 0.5 US gallons/hr (psi) 0.5. RP-3 kerosene, the sole fuel used in this study, is delivered at room temperature straight into the cavity through these centrifugal nozzles. A nozzle flow characteristic test was conducted to establish the relationship between fuel flow rate and fuel injection pressure, as shown in **Figure 4**. This test was carried out to ensure the reliability and accuracy of the experiment. Consequently, the adjustment of supply pressure allows for precise control of the fuel mass flow rate. The detailed

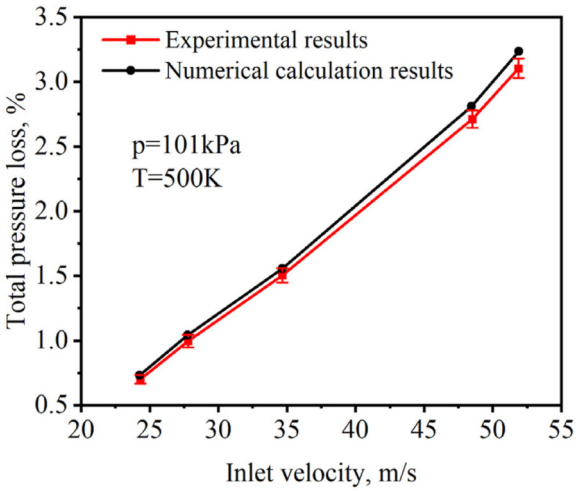

FIGURE 7 | The variation of the total pressure loss with the inlet velocity.

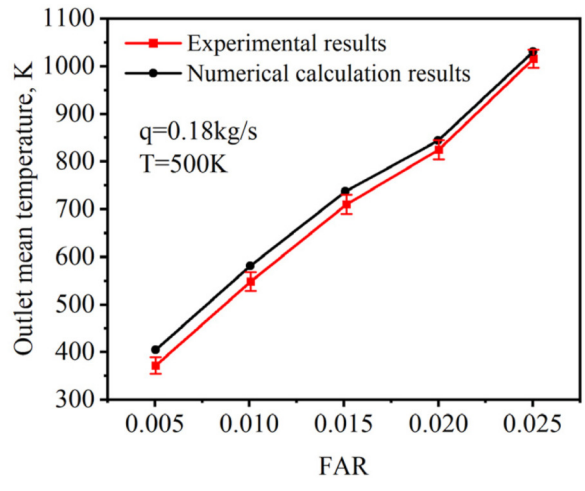

FIGURE 8 | The variation of the outlet mean temperature with the FAR.

properties of RP-3 kerosene, determined using the GB/T-test method, are presented in **Table 1**.

Igniter, voltage generator and semiconductor ignition nozzle are part of the ignition system. The ignition system features 20 joules ignition energy and 14 Hz ignition frequency. A direct ignition method is used to ignite the combustible mixture. The ignition is turned on simultaneously with the two ignitors, which are located at the two and ten o'clock positions. NI acquisition unit and computer are both part of data acquisition system and serve to capture and process temperature data. NI acquisition unit is employed to gather both inlet and outlet temperatures, ensuring a precision level within a range of 0.5% uncertainty.

This article concentrates on the experimental investigation of the of MTVC's ignition and blowout performance at low pressure. The working conditions are displayed in **Table 2**.

The selected pressure values (e.g., 35.3 kPa, 51.3 kPa) correspond to typical flight altitudes of approximately 8,000 m and 6,000 m, respectively, based on the International Standard Atmosphere. These conditions are representative of high-altitude relight scenarios for turboshaft engines, as referenced in prior studies [40].

Experiment Uncertainty Analysis

The uncertainties in this experiment, which are reflected in the Fuel-Air Ratio (FAR) within the cavity, are primarily attributed to the inlet parameters and fuel mass flow rate. These uncertainties include:

Fuel Flow Characteristic Experiment: A fuel flow characteristic experiment was conducted specifically for the centrifugal nozzles used in the study. The experiment established the relationship between fuel flow and injection pressure, as depicted in **Figure 4**. The calculated uncertainty for this relationship is 0.15%.

Instrument Error in Inlet Parameters Measurement: Several instruments were employed for measuring inlet parameters, each introducing a certain degree of error, as shown in **Table 3**.

These instrument errors should be taken into account when analyzing the results of the ignition and Lean Blowout (LBO) experiments to ensure accurate and reliable findings.

The desirable uncertainties of experiment results are computed based on uncertainties of variables used in the measurement using the Kline and McClintock method [42].

According to mathematical assumptions, the measured parameter (X) exhibits the following functional relationship with the directly measured parameters x_1, x_2, …, x_n as shown in **Equation 1**.

$$X = f(x_1, x_2, \cdots x_n) \tag{1}$$

Let ε_X be the measurement uncertainty (X) and $\varepsilon_{x_1}, \varepsilon_{x_2}, \ldots, \varepsilon_{x_n}$ be the dependent parameters uncertainties (x_n). Thus, uncertainty in the measurement is defined as

$$\varepsilon_X = \sqrt{\left(\frac{x_1}{X}\frac{\partial f}{\partial x_1}\varepsilon_{x_1}\right)^2 + \left(\frac{x_2}{X}\frac{\partial f}{\partial x_2}\varepsilon_{x_2}\right)^2 + \cdots + \left(\frac{x_n}{X}\frac{\partial f}{\partial x_n}\varepsilon_{x_n}\right)^2} \tag{2}$$

Based on air and fuel inlet mass flow rates, total ignition FAR is defined as shown in **Equation 3**.

$$f_{ig} = W_{fuel} / W_{air} \tag{3}$$

where W_{fuel} is fuel mass flow rate when combustor is successfully ignited, kg/s, W_{air} is air mass flow rate for ignition case, kg/s.

Global ignition equivalence ratio uncertainty from **Equation 2** is defined as shown in **Equation 4**.

$$\varepsilon_{f_{ig}} = \sqrt{\left(\varepsilon_{w_{fuel}}\right)^2 + \left(-\varepsilon_{w_{air}}\right)^2} \tag{4}$$

Therefore, root mean square of $\varepsilon_{w_{air}}$ and $\varepsilon_{w_{fuel}}$ is used to calculate overall ignition FAR measurement's total uncertainty $\varepsilon_{f_{ig}}$, and final calculation result of $\varepsilon_{f_{ig}}$ is 1.01%.

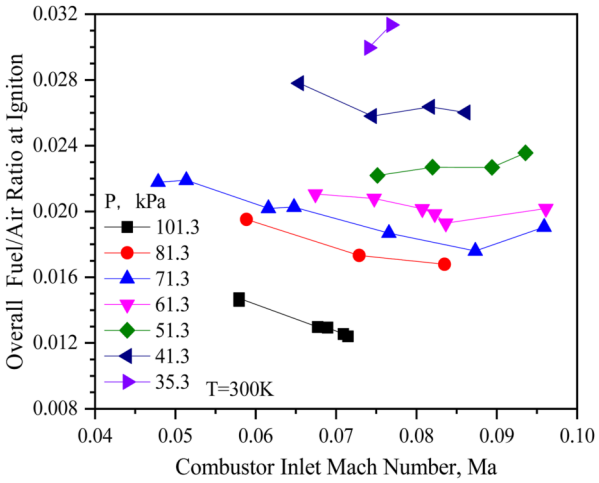

FIGURE 9 | Implication of pressure and Mach number on ignition performance.

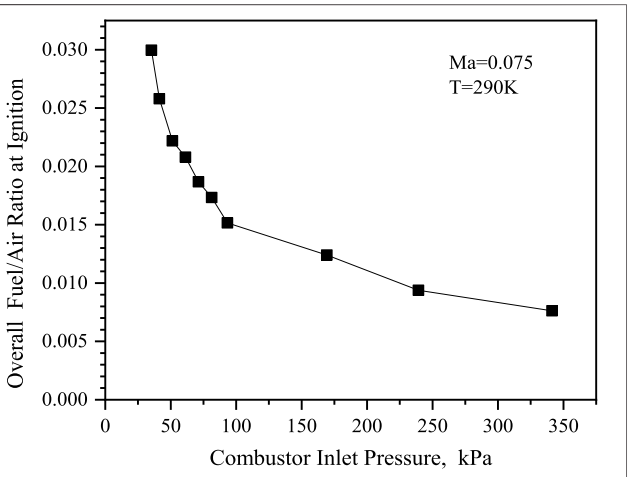

FIGURE 10 | Implication of inlet pressure on ignition performance.

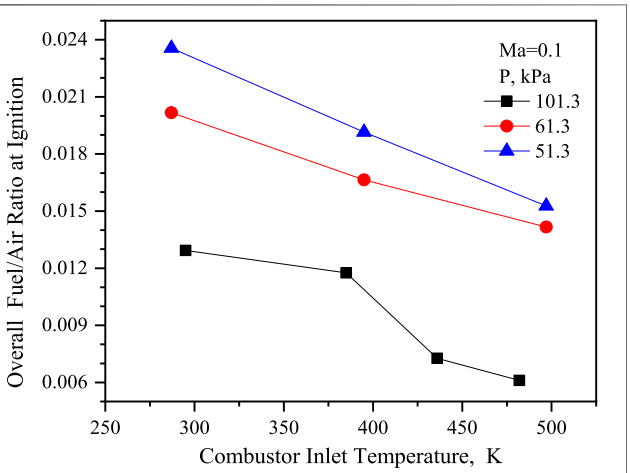

FIGURE 11 | Implication of inlet temperature on ignition performance.

NUMERICAL CALCULATION METHODS AND FEASIBILITY VERIFICATION

Numerical Calculation Methods

Numerical simulation in this work is done using commercial software named Fluent. A standard k-ε turbulence model is used to numerically simulate the turbulent motion in the cavity of the MTVC. The finite volume method is utilized to discretize the momentum equations and steady state continuity in the computing domain. A second-order upwind format is used to discretize the convective and diffusive terms. The SIMPLE algorithm is used for the pressure-velocity coupling. In numerical calculations, air can be considered as an uncompressible gas. **Figure 5** shows the inlet boundary of the combustor is configured as mass flow inlet, while its outlet is configured as pressure outlet. Side walls are set up as symmetry surfaces. Non-premixed combustion model close to the actual combustion situation in the cavity is chosen. The nozzle type is cone and the fuel spray cone angle is set to 80°. Kerosene-liquid ($C_{12}H_{23}$) is used for the fuel. The initial temperature of the fuel is 300 K and the fuel particle type is droplet.

Due to the complex structure of the MTVC, the computational is simplified to 1/5 and divided using an unstructured grid. The grid independence test uses six different grid numbers: G1 = 2.01 million, G2 = 2.71 million, G3 = 3.27 million, G4 = 4.02 million, G5 = 5.04 million, and G6 = 5.99 million. By comparing the velocity distributions in different height directions in the cavity on the Z = 0 cross-section, the results are shown in **Figure 6**. For the grids of 5.04 and 5.99 million, the trends of the velocity distributions and the magnitudes of the velocities at each place are essentially comparable. This suggests that after the number of grids reaches 5.04 million, the flow characteristics may be anticipated with stability. Therefore, the numerical simulation investigation in this work is conducted using 5.04 million grids.

Feasibility Verification

At an inlet pressure of 101 kPa and a temperature of 300 K, **Figure 7** displays experimental results and numerical calculation results of the variation of the total pressure loss with the inlet velocity. The total pressure loss increases as the inlet velocity rises for both approaches. The total pressure loss of numerical calculation results comes out to be marginally greater than the experimental results; the minimum is 3.9% and the maximum is 4.5%.

At an inlet mass flow rate of 0.18 kg/s and a temperature of 500 K, **Figure 8** displays the experimental results and numerical calculation results of the variation of the outlet mean temperature with the FAR. The outlet mean temperature increases with an increase in the FAR under both approaches. The numerical calculation results yielded an outlet mean temperature that is greater than the experimental results, with a maximum temperature of 1000 K. When the FAR is low, the discrepancy between the numerical calculations and the experimental results

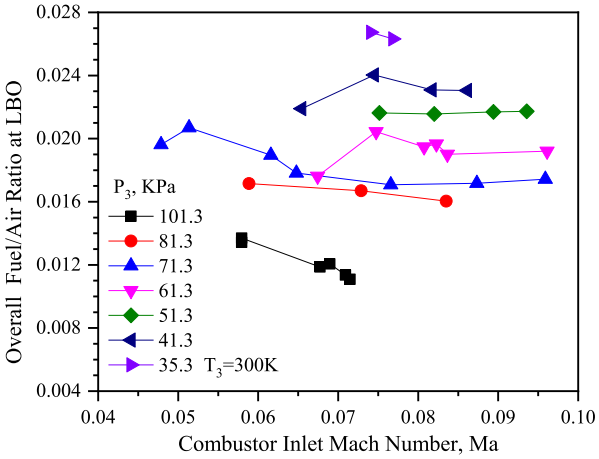

FIGURE 12 | Implication of pressure and Mach number on LBO performance.

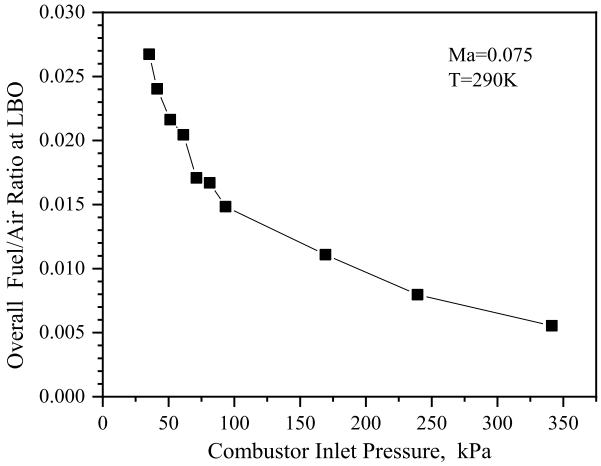

FIGURE 13 | Implication of inlet pressure on LBO performance.

is greatest, often within an 8.3% range. The experimental results and the numerical calculation results, however, are becoming closer and closer as the FAR rises. The discrepancy is at its lowest, 0.9%, when the FAR hits 0.025.

In conclusion, through the analysis of the experimental results and numerical calculation results of the total pressure loss and outlet mean temperature of the combustor, the difference of the total pressure loss is in the range of 3.9%–4.5%, and the minimum difference of the outlet mean temperature is 0.9%. It is evident that the numerical calculation methods used in this paper is effective, feasible and reliability.

RESULTS AND DISCUSSIONS

Ignition Performance

Ignition performance of aircraft engine is often described by the range of flight circumstances in which ignition is quickly and consistently achieved during ground starts, and combustion can be restarted after flameout at high altitude. The fuel flow rate was steadily raised while the inlet air velocity and temperature were maintained during the ignition experiment. Successful ignition is defined as a temperature rise in the combustor exceeding 80 ˚C. This threshold was selected based on the thermal inertia of the combustor liner and prior experimental studies [5, 12], ensuring a clear distinction between successful ignition and transient heating. The criterion remains consistent across different pressures, although the temperature rise magnitude varies due to changes in heat release rates. **Figure 9** illustrates impact of pressure and Mach number on ignition performance. The experiment maintained a constant inlet air temperature of 300 K and varied inlet total pressure from 35.3 to 101.3 kPa, while inlet Mach number ranged from 0.045 to 0.1. The results show that ignition FAR tends to decrease and then increase as Mach number increases. This suggests that both low and high Mach numbers have a negative effect on ignition. This is primarily due to low air mass flow rate and low fuel mass flow rate required for ignition at low Mach numbers. However, for centrifugal nozzles, small fuel mass flow rate results in low supply pressure, which hinders fuel atomization, evaporation, mixing, and ultimately ignition. On the other hand, at high Mach numbers, the air mass flow rate is high, resulting in a high velocity that easily blows out the flame, compromising flame stability. Consequently, the ignition FAR also increases at these high Mach numbers. The range of ignitable velocities narrows as the pressure drops, but the ignition FAR rises. At a pressure of 35.3 kPa at constant temperature, corresponding to an altitude of nearly 8,000 m, the combustor can be successfully ignited. But only two Mach numbers can be ignited, and the FAR is nearly 0.032, much higher than the ignition FAR of 0.012 at constant temperature of 101 kPa. This demonstrated how detrimental a pressure decrease is to ignition. **Figure 9** provides a clear illustration of these findings.

Figure 10 depicts the implication of inlet pressure on ignition performance. The combustor inlet temperature was 290 K, inlet velocity was 0.075 Ma, and inlet pressure ranged from 35.3 to 350 kPa in this test. It can be seen that ignition performance considerably improves as combustor inlet pressure rises, with ignition FAR dropping from 0.03 to 0.008 as inlet pressure rises from 35.3 kPa to 350 kPa. According to the slope of the curve, after the inlet pressure is below 101 kPa, ignition FAR rises rapidly as pressure decreases, indicating that ignition is becoming increasingly difficult. While inlet pressure is above 101 kPa, with the increase of pressure, the trend of ignition FAR decreases more slowly, indicating that after pressure increases to a certain value, the promotion effect on ignition is decreasing. From fuel and air mixing point of view, this is primarily because at the same inlet velocity and temperature, the increase in inlet pressure means an increase in air density. On the one hand, this increases the aerodynamic resistance of

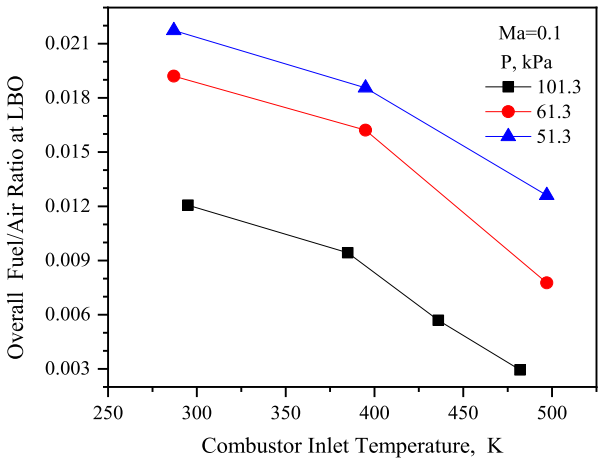

FIGURE 14 | Implication of inlet temperature on LBO performance.

the air to the fuel particles and reduces the penetration of the fuel, making the fuel more concentrated in the cavity and locally relatively fuel rich. This results in more fuel evaporating in the cavity to form the air phase fuel, allowing the required fuel to air ratio for ignition to be achieved more quickly (residual air coefficient close to 1) and facilitating ignition. On the other hand, with inlet pressure increases, air mass flow rate increases. Nozzle injection pressure must be raised in order to increase fuel flow rate in order to reach the minimum FAR necessary for ignite. This aids in enhancing fuel atomization process so that fuel evaporates promptly and combines with air to create a combustible combination that is also beneficial for ignition. In terms of chemical reaction dynamics, an increase in pressure increases the density of air per unit volume, which means that the concentration of reactants increases. The rate of chemical reaction is therefore accelerated and flame propagation rate is increased, which also facilitates ignition. Therefore, ignition FAR decreases with increasing inlet pressure.

Figure 11 depicts implication of inlet temperature on ignition performance. In this experiment, combustor inlet Mach number was 0.1, inlet pressures were 51.3, 61.3 and 101.3 kPa respectively, and inlet temperatures ranged from 283 to 500 K. It is observed that increase in temperature also has significant effect on ignition performance. As temperature climbs and pressure is at 101.3 kPa,

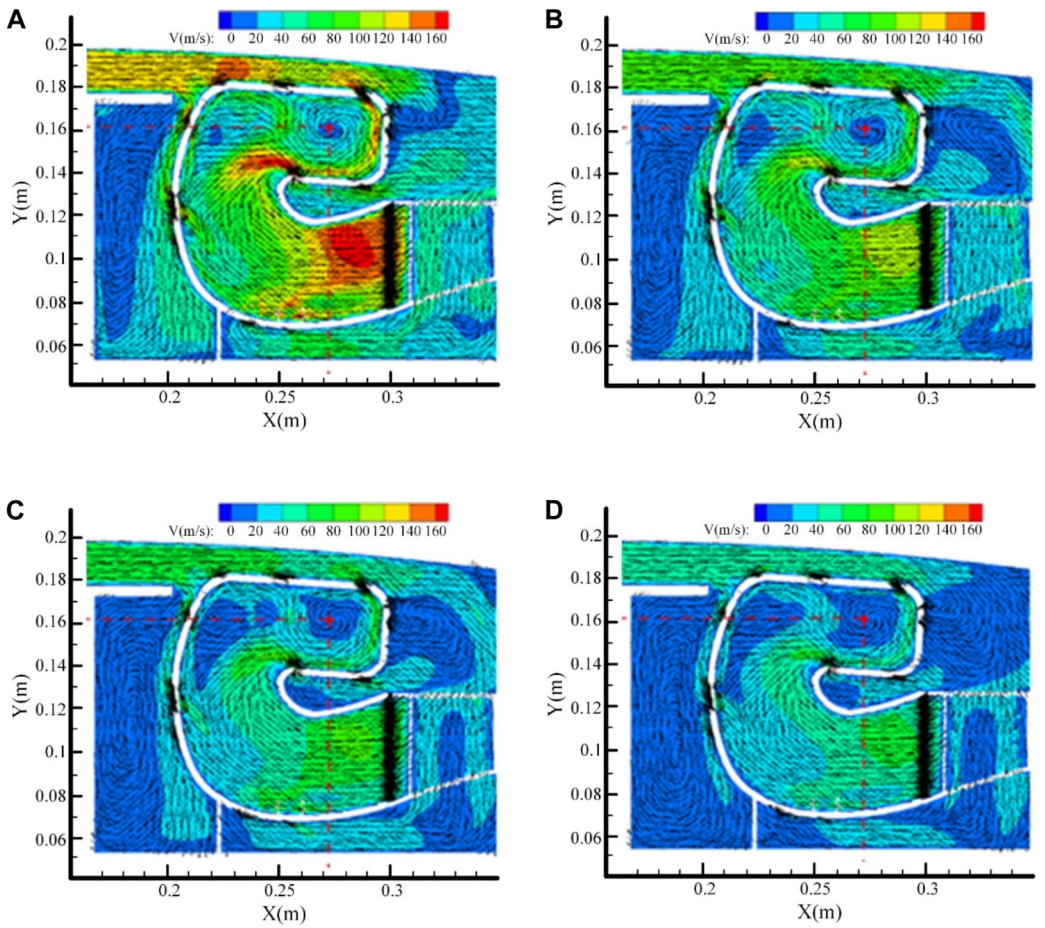

FIGURE 15 | The unreactive flow field at different pressures. **(A)** 0.04 MPa. **(B)** 0.06 MPa. **(C)** 0.08 MPa. **(D)** 0.1 MPa.

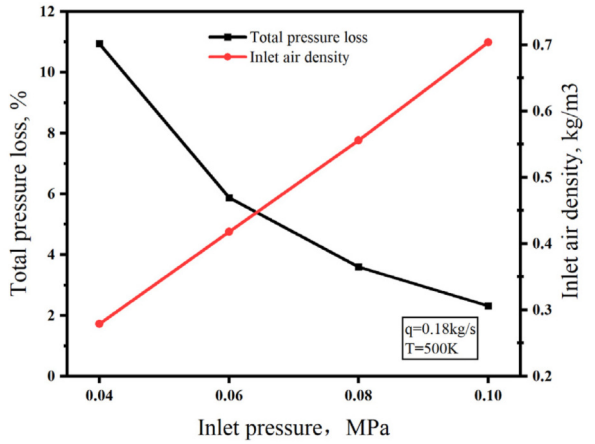

FIGURE 16 | The variation of total pressure loss and the variation of inlet air density at different pressures.

ignition FAR reduces from 0.013 to 0.006. As temperature climbs and pressure is at 51.3 kPa, it decreases from 0.023 to 0.016. This is mostly due to the fact that when temperature climbs and the intensification of the thermal movement of the molecules will cause the initial chemical reaction rate of the combustible mixture to accelerate. As a result, there is an increase in flame propagation and a decrease in the amount of heat dissipated, which facilitates the formation of a core fire mass. In addition, when temperature rises, fuel atomization quality improves and the rate of evaporation increases. More fuel vapor is produced and the rate of fuel evaporation grows quicker with increased evaporation. As a result, it will be simpler to light the FAR nearer to the igniter since it will be closer to the ignition point. Despite the increase in temperature to 500 K, the ignition FAR at 51.3 kPa is higher than that at 101.3 kPa and 290 K. This indicated that the detrimental effect on ignition caused by the reduced pressure is not compensated for by the increase in temperature. This is mostly caused by the lower pressure and lower oxygen concentration per unit volume, which in turn affects the reaction rate and fuel consumption.

In conclusion, the ability to ignite is weakly influenced by Mach number, while the ability to ignite is more strongly influenced by pressure and temperature increases, which can dramatically reduce the ignition FAR.

These experimental trends can be mechanistically explained by the CFD simulations presented in Section *Numerical Results*. Under lower pressures, the reduced fuel residence time and lower local oxygen concentration impede fuel-air mixing and reaction rates, thereby elevating the ignition FAR. Furthermore, the vortex stability within the cavity, as visualized in **Figure 13**, is compromised at higher Mach numbers, leading to increased flame susceptibility to blowout.

Lean Blowout Performance

The inlet velocity and temperature were held constant throughout the blowout experiment. The combustor was thought to be blowout if the fuel flow rate was progressively reduced and the burner temperature dropped. **Figure 12** depicts implication of pressure and Mach number on LBO performance. In this experiment, combustor inlet air temperature was kept at 300 K, inlet total pressure was in the range of 35.3–101.3 kPa, and inlet Mach number was in the range of 0.045–0.1. The variation of blowout FAR with Mach number demonstrates a pattern characterized by an initial rise, followed by a decline, and ultimately reaching a point of stabilization. At a constant temperature of 101 kPa, the blowout FAR is around 0.012. The inlet pressure at 35.3 kPa is much higher than 101 kPa, as high as 0.027, indicating that the reduction in pressure is also detrimental to the LBO performance. In addition, the speed boundary of the blowout also decreases with increasing pressure.

Figure 13 depicts the implication of inlet pressure on LBO performance. In this experiment, the inlet pressure varied from 35.3 to 350 kPa, inlet velocity was 0.075 Ma, and inlet temperature was 290 K. The blowout FAR drops noticeably as inlet pressure rises, going from 0.027 to 0.006 as inlet pressure rises from 35.3 kPa to 350 kPa. The slope of curve shows that as pressure decreases, the blowout FAR rises rapidly, indicating that the lower the pressure, the easier it is to blowout. And after the pressure at 101 kPa, with increase in pressure, blowout FAR decreases more slowly, indicating that pressure on the LBO performance improvement has a certain range. From the analysis of effect of pressure on ignition performance can be known, inlet pressure increases, it will make the pneumatic resistance increase. The nozzle pressure drops increase to change the atomization performance of fuel, oxygen concentration in the unit volume increases to improve flame propagation speed and chemical reaction rate, spark energy will also increase. These factors together can make the flame easier to stabilize and the LBO performance is improved. Recent experimental studies on air-cooled bluff-body flameholders have also demonstrated that optimized cooling air jet arrangements can extend the LBO limits and enhance flame stability under sub-atmospheric conditions [40, 43]. This supports the importance of flow and thermal management in maintaining vortex stability near the LBO boundary.

Figure 14 depicts the implication of inlet temperature on LBO performance. In this experiment, combustor inlet Mach number was 0.1, inlet pressures were 51.3, 61.3 and 101.3 kPa respectively, and inlet temperatures ranged from 283 to 500 K. It can be seen that increase in temperature and rapid decrease in blowout FAR, which plays a crucial implication on LBO performance. This is also mainly because an increase in temperature results in a faster initial chemical reaction rate of combustible mixture, a faster flame propagation rate, a higher quality of atomization of fuel and a faster evaporation rate.

NUMERICAL RESULTS

The results of the above tests demonstrate a significant deteriorate in ignition and blowout performance under sub-atmospheric pressure. In order to provide sufficient support for the test

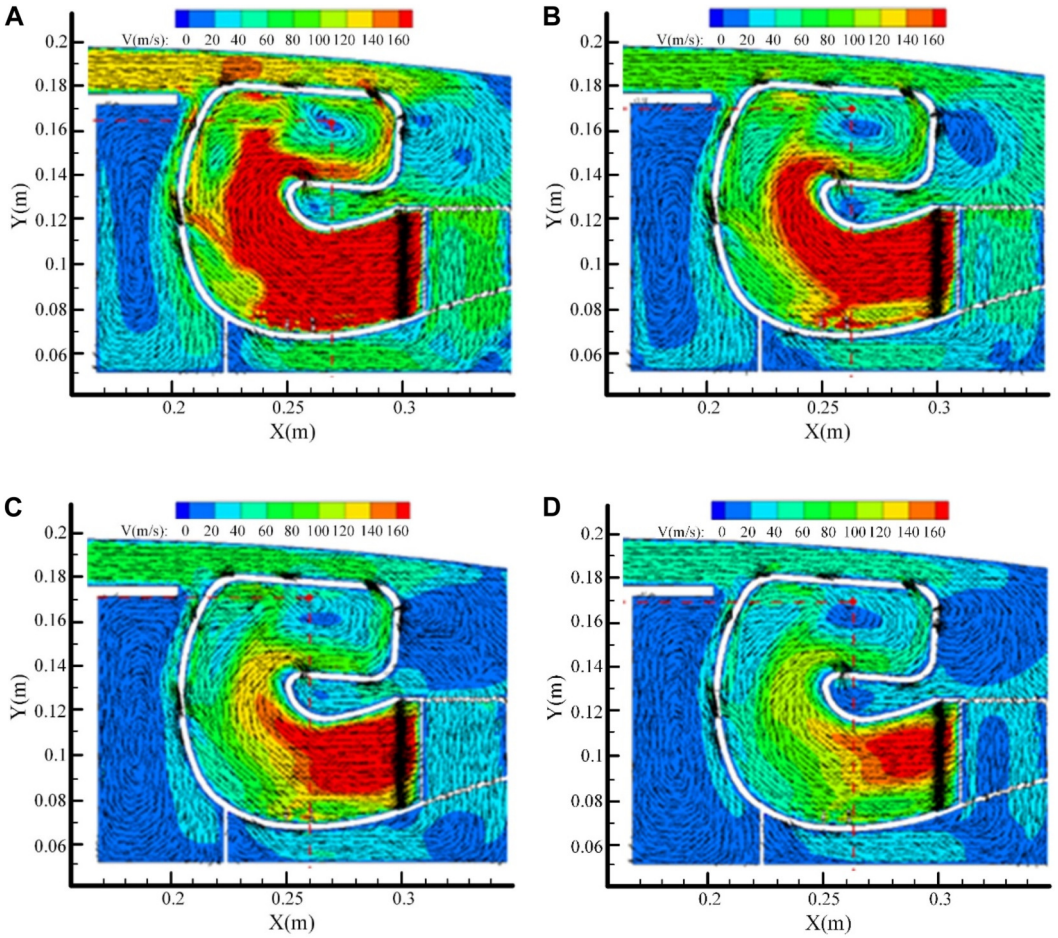

FIGURE 17 | The reactive flow field at various pressures. **(A)** 0.04 MPa. **(B)** 0.06 MPa. **(C)** 0.08 MPa. **(D)** 0.1 MPa.

results and the analysis process, numerical calculations were performed for the non-reactive flow field structure, total pressure loss, as well as the reactive flow field structure, temperature distribution, and component distribution of the MTVC, at an inlet mass flow rate of 0.18 kg/s, an inlet temperature of 500 K, and four inlet pressures of 0.04, 0.06, 0.08, and 0.1 MPa.

Unreactive Flow Simulations

The unreactive flow field at different pressures is seen in **Figure 15**. There is a stable and complete single vortex structure residing in the cavity, and the vortex structure is stable as the pressure fluctuates. The dimensions and center position of the vortex structure essentially stay the same as the pressure drops, but the inlet velocity at each site significantly increases.

The variation of total pressure loss at different pressures is shown in **Figure 16**. The total pressure loss in the combustor rises from 2.35% to 11.04%, approximately almost 370%, as the inlet pressure drops from 0.1 MPa to 0.04 MPa. The drop in pressure is the primary cause of the rise in the overall pressure loss. The combustor experiences a large increase in velocity everywhere. On the one hand, the combustor's high-speed airflow in the curve-shaped wall makes it simple for the air to split, creating a large number of tiny vortex structures, which will increase the loss due to their dissipation. On the other hand, the loss will rise as a result of the high-speed air flow passing through the different inlet holes, which will enlarge the vortex between the jet and the wall. It is simple to engage the hot air in this increasing vortex structure, which leads to flame quenching. Furthermore, when the velocity increases, the friction between the jet and the wall will also increase, resulting in a rise in energy loss.

The variation of inlet air density at different pressures is shown in **Figure 16**. The inlet air density decreased by almost 60%, from 0.71 to 0.28, when the inlet pressure dropped from 0.1 MPa to 0.04 MPa. The oxygen concentration per unit volume decreases as air density decreases. However, the combustion chemical reaction in the combustor is mainly realized by the collision between the fuel and the oxygen molecules. Therefore, reducing the concentration of oxygen per unit volume limits the quantity of direct effective

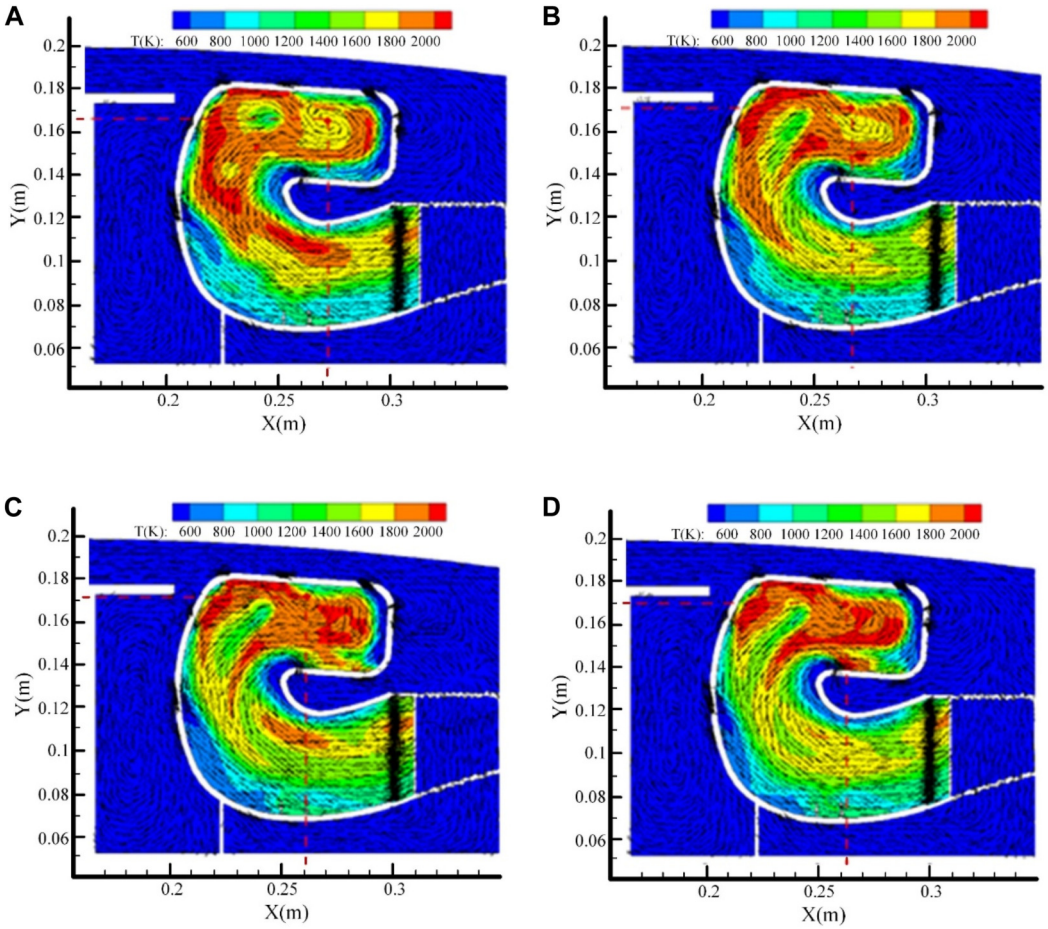

FIGURE 18 | The temperature distribution at various pressures. **(A)** 0.04 MPa. **(B)** 0.06 MPa. **(C)** 0.08 MPa. **(D)** 0.1 MPa.

collisions that occur between oxygen molecules and fuel particles, hence lowering the pace of chemical reaction. This reduces the quantity of fuel used per unit of time and reduces the temperature of the fuel-air mixture due to a decrease in the rate of exothermic heat release. These factors are harmful to the ignition and flame stability of the combustor.

Reactive Flow Simulations

The reactive flow field at various pressures is seen in **Figure 17**. Reducing the pressure from 0.1 MPa to 0.06 MPa results in essentially the same flow field structure, vortex center position, and vortex size. On the other hand, the vortex center location is closer to the geometric center of the cavity and the vortex structure is fuller at 0.04 MPa. In every area of the combustor, the inflow velocity rises as the pressure drops.

The temperature distribution at various pressures is depicted in **Figure 18**. When the pressure is 0.1 MPa, the fuel is basically consumed completely in the upstream of the combustor. The high temperature zone above 2000 K is mainly distributed in the cavity and part of the mainstream area. As the pressure decreases, the temperature in the cavity decreases to below 2000 K, and the temperature in the return area decreases to 1800 K. The high temperature zone above 2000 K is distributed in the downstream of the cavity. This is mainly because of the pressure reduction, the combustor velocity increases in all areas, the fuel residence time decreases, the cavity combustion evaporation rate decreases. Most of the fuel leaves the cavity, which makes the high temperature zone shift to the downstream of the combustor. Concurrently, the cavity experiences a reduction in temperature due to insufficient fuel combustion. Additionally, all the fuel is fed into the cavity, which has an impact on the atomization and evaporation of newly added fuel.

The distribution of $C_{12}H_{23}$ concentration at various pressures is depicted in **Figure 19**. The distribution of $C_{12}H_{23}$ in the cavity increases with decreasing pressure, suggesting that the fuel is getting harder to consume. This is mainly because, as the pressure decreases, the cavity's velocity rises and the oxygen concentration per unit volume falls, causing the fuel residence time and fuel evaporation rate to drop.

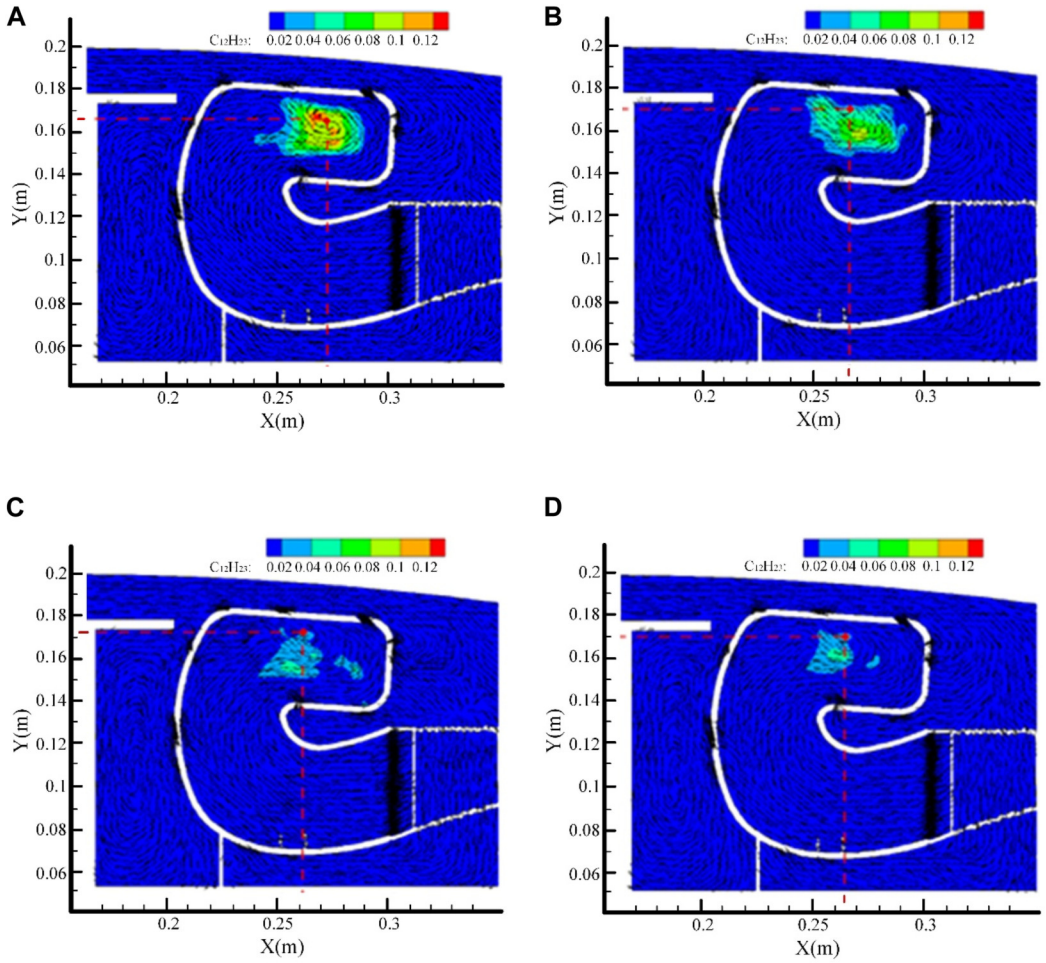

FIGURE 19 | The distribution of $C_{12}H_{23}$ concentration at various pressures. **(A)** 0.04 MPa. **(B)** 0.06 MPa. **(C)** 0.08 MPa. **(D)** 0.1 MPa.

CONCLUSION

The most significant finding of this study is that successful ignition can still be achieved at a pressure as low as 35.3 kPa, although the required fuel-to-air ratio increases substantially. This result highlights the robust ignition capability of the mixed-flow trapped vortex combustor under extreme sub-atmospheric conditions. Performance of LBO and ignition are examined at sub-atmospheric pressure environment, and numerical simulations of unreactive flow and reactive flow have been completed. The following findings are arrived at:

As pressure decreases, the ignition FAR increases and the range of ignitable velocities decreases. Under constant temperature conditions, the ignition pressure of the combustor can reach 35.3 kPa, and the corresponding altitude is close to 8,000 m. However, the ignition FAR is close to 0.032, which is much higher than the FAR of 0.012 at 101.3 kPa, indicating that the decrease in pressure is very detrimental to ignition. Meanwhile, as pressure decreases, the LBO FAR keeps increasing.

There is also a significant increase in ignition performance with increasing temperature. At 101.3 kPa, ignition FAR decreases from 0.013 to 0.006 as temperature increases, and at 51.3 kPa, ignition FAR decreases from 0.023 to 0.016 as temperature increases. Ignition FAR at 51.3 kPa was higher than that at 101.3 kPa and 290 K, indicating that the detrimental effect on ignition caused by the reduced pressure was not compensated for by the climbs in temperature. As the temperature climbs, the LBO FAR decreases rapidly, which plays a crucial implication on the ignition performance.

As Mach number increases, ignition FAR tends to decrease and then increase, but not particularly significantly. Simultaneously, The LBO FAR change pattern with increasing Mach number indicates that it initially rises, then declines, and eventually stabilizes.

A stable vortex structure is created in the cavity. The size of the vortex structure and the position of the vortex center basically remained unchanged with the decrease in pressure, but there is a significant increase in the inlet velocity at each location. As the inlet pressure decreases from 0.1 MPa to 0.04

MPa, the total pressure loss of the combustor increases from 2.35% to 11.04%, and the inlet air density of the combustor decreases from 0.71 to 0.28.

When the pressure is 0.1 MPa, the fuel is basically consumed completely in the upstream of the cavity, and the high-temperature zone above 2000 K is mainly distributed in the cavity and part of the main flow area. As the pressure decreases, the high temperature zone above 2000 K is distributed in the downstream of the combustor.

DATA AVAILABILITY STATEMENT

The original contributions presented in the study are included in the article/supplementary material, further inquiries can be directed to the corresponding authors.

AUTHOR CONTRIBUTIONS

QL: Conceptualization, Methodology, Formal Analysis, Investigation, Data Curation, Writing – Original Draft, Visualization. Led the experimental campaign and CFD simulations, analyzed ignition/LBO data under sub-atmospheric conditions, and drafted the manuscript. PJ: Software, Validation, Formal Analysis, Resources. Developed and optimized CFD models for annular mixed-flow TVC, performed turbulence-chemistry interaction simulations, validated results against experimental data. HH: Investigation, Resources, Data Curation. Designed and executed sub-atmospheric pressure experiments, established optical diagnostics for flame stabilization analysis, curated critical datasets. ZW: Methodology, Validation, Writing – Review and Editing. Contributed to combustion mechanism validation, interpreted lean blowout dynamics, revised technical content. XH: Supervision, Project Administration, Funding Acquisition, Writing – Review and Editing. Oversaw research direction, secured funding, provided critical review of combustion performance interpretation. All authors contributed to the article and approved the submitted version.

FUNDING

The author(s) declared that financial support was received for this work and/or its publication. This work was supported by the Funding of Nanchang Hangkong University Doctoral Initiation through No. EA202106307, Jiangxi Provincial Education Department Science and Supported by Jiangxi Provincial Natural Science Foundation No. 20252BAC240327 and Nanchang Hangkong University Graduate Student Innovation Special Fund Project through No. YC2024-031.

CONFLICT OF INTEREST

The author(s) declared that this work was conducted in the absence of any commercial or financial relationships that could be construed as a potential conflict of interest.

GENERATIVE AI STATEMENT

The author(s) declared that generative AI was not used in the creation of this manuscript.

Any alternative text (alt text) provided alongside figures in this article has been generated by Frontiers with the support of artificial intelligence and reasonable efforts have been made to ensure accuracy, including review by the authors wherever possible. If you identify any issues, please contact us.

REFERENCES

1. Linassier G, Viguier C, Verdier H, Lecourt R, Linassier G, Lavergne G, editors. Experimental Investigations of the Ignition Performances on a Multi-Sector Combustor Under High Altitude Conditions. *50th AIAA Aerospace Sciences Meeting Including the New Horizons Forum and Aerospace Exposition* (2012). p. 1–9.
2. Bents DJ, Mockler T, Maldonado J, Harp JJL, King JF, Pcjst S. *Propulsion System for Very High Altitude Subsonic Unmanned Aircraft* (1998). p. 100–15.
3. Read RW. *Experimental Investigations into High-Altitude Relight of a Gas Turbine* (2008).
4. Okai K, Himeno T, Watanabe T, Kobayashi H, Taguchi H. Investigation of Combustion and Altitude-Ignition Performance of a Small hydrogen-Fueled Reversed-Flow Turbine Combustor. In: *52nd Aerospace Sciences Meeting*. Reston, VA: American Institute of Aeronautics and Astronautics (AIAA) (2014). p. 1–9.
5. He XM, Hang QX, Tan HY. An Investigation on Ignition Performance of a Catalytic Igniter at High Altitude. *J Aerospace Power* (1997) 12(2):146–68.
6. Hirst R, Sutton DJC. The Effect of Reduced Pressure and Airflow on Liquid Surface Diffusion. *Combustion and Flame* (1961) 5:319–30. doi:10.1016/0010-2180(61)90113-4
7. Most JM, Mandin P, Chen J, Joulain P, Durox D, Fernande-Pello AC, editors. Influence of Gravity and Pressure on Pool Fire-Type Diffusion Flames. *Symposium (International) on Combustion* (1996). p. 1311–7.
8. Wieser D, Jauch P, Willi U. The Influence of High Altitude on Fire Detector Test Fires. *Fire Saf J* (1997) 29(2-3):195–204. doi:10.1016/s0379-7112(96)00042-2
9. Jun F, Yu CY, Ran T, Qiao LF, Zhang YM, Wang J. The Influence of Low Atmospheric Pressure on Carbon Monoxide of n-heptane Pool Fires. *J Hazard Mater* (2008) 154(1-3):476–83. doi:10.1016/j.jhazmat.2007.10.058
10. Fang J, Tu R, Guan J-f, Wang J-j, Zhang Y-mJF. Influence of Low Air Pressure on Combustion Characteristics and Flame Pulsation Frequency of Pool Fires. *Fuel* (2011) 90(8):2760–6. doi:10.1016/j.fuel.2011.03.035
11. Brookes S, Moss JJC. Flame. Measurements of Soot Production and Thermal Radiation from Confined Turbulent Jet Diffusion Flames of Methane. *Combustion and Flame* (1999) 116(1-2):49–61. doi:10.1016/s0010-2180(98)00027-3
12. Brookes S, Moss J. Predictions of Soot and Thermal Radiation Properties in Confined Turbulent Jet Diffusion Flames. *Combustion and Flame* (1999) 116(4):486–503. doi:10.1016/s0010-2180(98)00056-x
13. Beltrame A, Porshnev P, Merchan-Merchan W, Saveliev A, Fridman A, Kennedy L, et al. Soot and NO Formation in methane–oxygen Enriched Diffusion Flames. *Combustion and Flame* (2001) 124(1-2):295–310. doi:10.1016/s0010-2180(00)00185-1
14. Hsu KY, Goss L, Roquemore WMP. Characteristics of a Trapped-Vortex Combustor. *Power* (1998) 14(1):57–65. doi:10.2514/2.5266
15. Jiang P, He X. Ignition Characteristics of a Novel Mixed-Flow Trapped Vortex Combustor for Turboshaft Engine. *Fuel* (2020) 261:116430. doi:10.1016/j.fuel.2019.116430

16. Xing F, Wang P, Zhang S, Zou J, Zheng Y, Zhang R, et al. Experiment and Simulation Study on Lean Blow-Out of Trapped Vortex Combustor with Various Aspect Ratios. *Technol* (2012) 18(1):48–55. doi:10.1016/j.ast.2011.03.010
17. Kumar PE, Mishra DP. Numerical Simulation of Cavity Flow Structure in an Axisymmetric Trapped Vortex Combustor. *Technol.* (2012) 21(1):16–23.
18. Wu Z, Jin Y, He X, Xue C, Hong L. Experimental and Numerical Studies on a Trapped Vortex Combustor with Different Struts Width. *Appl Therm Eng* (2015) 91:91–104. doi:10.1016/j.applthermaleng.2015.06.068
19. Zeng Z, Du P, Wang Z, Li KJ. Technology. Combustion Flow in Different Advanced Vortex Combustors with/without Vortex generator. *Aerospace Sci Technol* (2019) 86:640–9. doi:10.1016/j.ast.2019.01.048
20. Jiang P, He X. Experimental Investigation of Flow Field Characteristics in a Mixed-Flow Trapped Vortex Combustor. *Aerospace Sci Technol* (2020) 96: 105533. doi:10.1016/j.ast.2019.105533
21. Jiang P, He X. Performance of a Novel Mixed-Flow Trapped Vortex Combustor for Turboshaft Engine. *Aerospace Sci Technol* (2020) 105: 106034. doi:10.1016/j.ast.2020.106034
22. Roquemore W, Shouse D, Burrus D, Johnson A, Cooper C, Duncan B, editors *Vortex Combustor Concept for Gas Turbine Engines. 39th Aerospace Sciences Meeting and Exhibit* (2001).
23. Burrus D, Johnson A, Roquemore W, Shouse D, editors. *Performance Assessment of a Prototype Trapped Vortex Combustor Concept for Gas Turbine Application. Turbo Expo: Power for Land, Sea, and Air*. American Society of Mechanical Engineer. (2001). p. 4–7.
24. Jin Y, He X, Jiang B, Wu Z, Ding G, Zhu Z, et al. Effect of Cavity-Injector/ Radial-Strut Relative Position on Performance of a Trapped Vortex Combustor. *Aerospace Sci Technol* (2014) 32(1):10–8. doi:10.1016/j.ast.2013.12.014
25. Li M, He X, Zhao Y, Jin Y, Ge Z, Sun Y. Dome Structure Effects on Combustion Performance of a Trapped Vortex Combustor. *Appl Energy* (2017) 208:72–82. doi:10.1016/j.apenergy.2017.10.029
26. Li M, He X, Zhao Y, Jin Y, Yao K, Ge Z. Performance Enhancement of a Trapped-Vortex Combustor for Gas Turbine Engines Using a Novel Hybrid-Atomizer. *Appl Energy* (2018) 216:286–95. doi:10.1016/j.apenergy.2018.02.111
27. Zhang R, Bai N, Fan W, Huang X, Fan X. Influence of Flame Stabilization and Fuel Injection Modes on the Flow and Combustion Characteristics of Gas Turbine Combustor with Cavity. *Energy* (2019) 189:116216. doi:10.1016/j.energy.2019.116216
28. Zhang R, Fan WJ. Flow Field Measurements in the Cavity of a Trapped Vortex Combustor Using PIV. *J Therm Sci* (2012) 21(4):359–67. doi:10.1007/s11630-012-0556-z
29. Zhang R, Fan W, Shi Q, Tan WJ. Combustion and Emissions Characteristics of Dual-Channel Double-Vortex Combustion for Gas Turbine Engines. *Appl Energy* (2014) 130:314–25. doi:10.1016/j.apenergy.2014.05.059
30. Zhang R, Fan W, Shi Q, Tan WJ. Structural Design and Performance Experiment of a Single Vortex Combustor with Single-Cavity and Air Blast Atomisers. *Aerospace Sci Technol* (2014) 39:95–108. doi:10.1016/j.ast.2014.08.017
31. Zhang R, Fan W, Xing F, Song S, Shi Q, Tian G, et al. Experimental Study of Slight Temperature Rise Combustion in Trapped Vortex Combustors for Gas Turbines. *Energy* (2015) 93:1535–47. doi:10.1016/j.energy.2015.09.122
32. Zelina J, Sturgess G, Shouse D. The Behavior of an Ultra-Compact Combustor (UCC) Based on Centrifugally-Enhanced Turbulent Burning Rates. In: *40th AIAA/ASME/SAE/ASEE Joint Propulsion Conference and Exhibit* (2004).
33. Zelina J, Shouse D, Hancock R, editors. Ultra-Compact Combustors for Advanced Gas Turbine Engines. *Turbo Expo: Power for Land, Sea, and Air* (2004).
34. Miranda Jr. P, Polanka MD. The Use of an Ultra-Compact Combustor as an Inter-Turbine Burner for Improved Engine Performance. In: *52nd Aerospace Sciences Meeting*. Reston, VA: American Institute of Aeronautics and Astronautics (AIAA) (2014). p. 2014–0458.
35. Erdmann TJ, Burrus DL, Gross JI, Shouse D, Neuroth C, Lynch A. Experimental Characterization of the Reaction Zone in an Ultra-Compact Combustor. In: *50th AIAA/ASME/SAE/ASEE Joint Propulsion Conference*. Reston, VA: American Institute of Aeronautics and Astronautics (AIAA) (2014). p. 2014–3630.
36. Briones AM, Sekar B, Shouse DT, Blunck DL, Thornburg HJ, Erdmann TJ, et al. Reacting Flows in Ultra-Compact Combustors with Combined-Diffuser Flameholder. *J Propulsion Power* (2015) 31(1):238–52. doi:10.2514/1.b35141
37. Jiang B, Jin Y, Liu D, Wu Z, Ding G, Zhu Z, et al. Effects of Multi-Orifice Configurations of the Quench Plate on Mixing Characteristics of the Quench Zone in an RQL-TVC Model. *Exp Therm Fluid Sci* (2017) 83:57–68. doi:10.1016/j.expthermflusci.2016.12.011
38. Straub DL, Casleton KH, Lewis RE, Sidwell TG, Maloney DJ, Richards GA. Assessment of Rich-Burn, Quick-Mix, Lean-Burn Trapped Vortex Combustor for Stationary Gas Turbines. *J Eng Gas Turbines Power* (2005) 127(1):36–41. doi:10.1115/1.1789152
39. Bucher J, Edmonds RG, Steele RC, Kendrick DW, Chenevert BC, Malte PC. The Development of a Lean-Premixed Trapped Vortex Combustor. *Turbo Expo Power Land, Sea, Air* (2003).
40. Chen Y, Fan Y, Han Q, Shan X, Bi Y, Deng YJ. The Influence of Cooling Air Jets on the Premixed Flame Structure and Stability of Air-Cooled Bluff-Body Flameholder. *Fuel* (2022) 310:122239. doi:10.1016/j.fuel.2021.122239
41. Chen Y, Fan Y, Xu L, Shan X, Han Q, Bai X, et al. Experimental and Numerical Study of Flow and Ignition and Lean Blowout Characteristics of Jet-Cooled Wall Flameholder in a Dual-Mode Combustor. *Aerospace Sci Technol* (2022) 122:107403. doi:10.1016/j.ast.2022.107403
42. Kline SJJME. Describing Uncertainties in Single-Sample Experiments. *Mech Eng* (1963) 75:3–8.
43. Zhang Z, Chen Y, Fan Y, Liu H, Haung YJAS. Technology. Experimental Study on the Combustion Performance of an Air-Cooled Afterburner with Varied Cooling Jet Conditions. *Aerospace Sci Technol* (2025) 167:110647. doi:10.1016/j.ast.2025.110647

NOMENCLATURE

MTVC mixed-flow trapped vortex combustion

TVC trapped vortex combustion

RQL rich-quench-lean

LBO lean blowout

FAR fuel to air ratio

Ma Mach number

P inlet pressure

T inlet temperature

$\mathbf{V_{in}}$ inlet velocity

q mass flow rate

$\boldsymbol{X}$ measured parameter

$\boldsymbol{x_n}$ measured independent parameter

$\boldsymbol{\varepsilon_X}$ measurement uncertainty

$\boldsymbol{\varepsilon_{x_n}}$ dependent parameters uncertainties

$\boldsymbol{f_{ig}}$ ignition fuel to air ratio

$\mathbf{W_{\boldsymbol{fuel}}}$ fuel mass flow rate, kg/s

$\mathbf{W_{\boldsymbol{air}}}$ air mass flow rate, kg/s

$\boldsymbol{\varepsilon_{f_{ig}}}$ ignition FAR uncertainty

$\boldsymbol{\varepsilon_{w_{air}}}$ air mass flow rate uncertainty

$\boldsymbol{\varepsilon_{w_{fuel}}}$ fuel mass flow rate uncertainty